# Isotopic variations in surface waters and groundwaters of an extremely arid basin and their responses to climate change

Yu Zhang[1], Hongbing Tan[1, *], Peixin Cong[1], Dongping Shi[1], Wenbo Rao[1], Xiying Zhang[2]

[1]School of Earth Sciences and Engineering, Hohai University, Nanjing 210098, China

[2]Qinghai Institute of Salt Lakes, CAS, Xining 810008, China

*** Corresponding author:** Hongbing Tan (tan815@sina.com)

## Abstract

Climate change accelerates the global water cycle. However, the relationships between climate change and hydrological processes in the alpine arid regions remain elusive. We sampled surface water and groundwater at high spatial and temporal resolution to investigate these relationships in the Qaidam Basin, an extremely arid area in the northeastern Tibetan Plateau. Stable H-O isotopes and radioactive $^{3}H$ isotope were combined with atmospheric simulations to examine hydrological processes and their response mechanisms to climate change. Contemporary climate processes and change dominate the spatial and temporal variations of surface water isotopes, specifically, the westerlies moisture transport and the local temperature and precipitation regimes. The spatial H-O isotopic compositions in the Eastern Kunlun Mountains showed a gradually depleted eastward pattern; while a reverse pattern occurred in the Qilian Mountains water system. Precipitation contributed significantly more to river discharge in the eastern basin (approximately 45%) than in the middle and western basin (10%–15%). Moreover, increasing precipitation and shrinking cryosphere caused by current climate change have accelerated basin groundwater circulation. In the eastern and southwestern Qaidam Basin, precipitation and meltwater infiltrate along preferential flow paths, such as faults, volcanic channels, and fissures, permitting rapid seasonal groundwater recharge and enhanced terrestrial water storage. However, compensating for water loss due to long-term ice and snow melt will be a challenge under projected increasing precipitation in the southwestern Qaidam Basin, and the total water storage may show a trend of increasing before decreasing. Great uncertainty about water is a potential climate change risk facing the arid Qaidam Basin.

## 1. Introduction

In the face of ongoing environmental changes, a thorough understanding of the hydrological cycle is a prerequisite for accurate trend forecasting, and helps to design efficient water resource management strategies. Over the past half century, climate change and more intense human activities have led to global water cycle acceleration and water resource redistribution at different scales (Huntington et al., 2006; Durack et al., 2012; Masson-Delmotte et al., 2021). For example, rapid warming has sharply expanded lakes in the Tibetan Plateau and shrunk them in the Mongolian Plateau (Zhang et al., 2017), and has also exacerbated the severe irrigation water shortage in parts of South Asia and East Asia (Haddeland et al., 2014). Moreover, warming is expected to reduce groundwater storage in the western United States (Condon et al., 2020). Currently, the climate in arid regions of northwestern China is changing from warm–dry to warm–wet (Zhang et al., 2021). The resulting uncertainties in water resources in arid alpine basins pose new challenges to understand the hydrological cycle and water resources. These key scientific issues can be addressed by investigating the spatial and temporal distribution and control mechanisms of surface water and groundwater resources within the basin under accelerating climate change.

The Tibetan Plateau, known as the "Third Pole", has complex cryospheric-hydrologic-geodynamic processes and is especially vulnerable to global warming (Zhang et al., 2017; Yao et al., 2022). The Qaidam Basin in the northeastern Tibetan Plateau is the area that has warmed the most in the entire Tibetan Plateau (Li et al., 2015; Kuang and Jiao, 2016; Yao et al., 2022). Since 1961, the average temperature of the basin has increased at an alarming rate of 0.53°C per decade (Wang et al., 2014), resulting in increased precipitation and cryospheric retreat (Song et al., 2014; Xiang et al., 2016; Zou et al., 2022; Wang et al., 2023). These changes have led to drastic spatial changes in surface water and groundwater storage, increasing runoff over wide areas (Jiao et al., 2015; Wei et al., 2021), and hydrological changes in the central and northern basin, such as the lakes expansion (Ke et al., 2022; Zhang et al., 2022). However, several questions remain to be answered: How are hydrological changes in the basin driven by climate change? What are the potential influences of these changes on the water resources of the basin? The dynamics of surface water and groundwater, which link precipitation and meltwater from high elevations with the low-lying lake basins, provide evidence of the effects of climate change on water cycle processes. The

Qaidam Basin is therefore an excellent site to reveal the mechanisms of global warming-induced responses to the hydrological cycle on the Tibetan Plateau.

The isotopes of hydrogen and oxygen are useful tracers for the water cycle and climate reconstruction. They can help elucidate the processes that control water cycle changes, thus providing scientific evidence for human adaptations and effects on future global changes (Craig, 1961; Dansgaard, 1964; Yao et al., 2013; Bowen et al., 2019; Kong et al., 2019; Zhu et al., 2023). Water isotope records provide key information on water flow, and they can compensate for the paucity of hydrometeorological, geological, and borehole data in hydrological research. Stable H-O isotopes and radioactive $^{3}H$ isotope have been widely applied to quantify surface water or groundwater recharge sources, interactions, budgets, and ages (Befus et al., 2017; Stewart et al., 2017; Moran et al., 2019; Bam et al., 2020; Rodriguez et al.,2021; Shi et al., 2021; Ahmed et al., 2022; Benettin et al., 2022). Previous researchers have also performed a substantial amount of work on using isotopes to delineate the water cycle in the Qaidam Basin (Xu et al., 2017; Xiao et al., 2017, 2018; Zhao et al., 2018; Tan et al., 2021; Yang and Wang, 2020; Yang et al., 2021). These studies have enhanced our understanding of aquifer properties in local regions and recharge mechanisms. However, past assessments of the water cycle in the Qaidam Basin have been constrained by the challenges of the harsh natural conditions and scarce hydrogeological data It is a great challenge to achieve a comprehensive elucidation of the basin-scale water cycle mechanism. Furthermore, seasonal recharge of the whole basin has not been systematically explored. Various hydrological, climatic, and hydrogeological conditions of the basin are caused by continuous changes in the topographical and tectonic spatial patterns; moreover, the hydrological effects exerted by anthropogenic climate change differ seasonally (Jasechko et al., 2014). Therefore, it is urgent to develop a comprehensive understanding of the basin water cycle and its seasonal changes. While carrying out a comprehensive assessment of differences in isotopic compositions of various potential recharge sources, it is fundamental to use the same technical methods for the systematic sampling and isotopic characterization of the basin.

In this study, we constrain the hydrological cycle of the Qaidam Basin and surrounding mountains using stable H-O and radioactive $^{3}H$ isotope data collected during the wet and dry seasons from eight study sites in major watersheds in the basin. The study aims are: 1) to elucidate the distribution pattern of surface water and groundwater isotopes in this alpine arid basin at various spatial and seasonal scales; 2) to identify and quantify the main components of the regional

89 water cycle, their timing and spatial heterogeneity; and 3) to reveal isotopic hydrological responses
90 to climate change and to predict the trend of the changes of Qaidam Basin water resources.

91 **2. Study area**

92 2.1. General features

93 The Qaidam Basin is a closed fault-depression basin in the northeastern Tibetan Plateau
94 surrounded by the Kunlun, Qilian and Altun Mountains (Figures 1a and 1b). The basin is one of
95 the four main basins in China with an area of approximately 250,000 $km^2$. It has a plateau
96 continental climate with a typical alpine arid inland basin characterized by drought. There are
97 significant temperature variations across the basin, and the mean annual temperature is less than
98 5 °C. Annual precipitation varies from 200 mm in the southeastern region to 15 mm in the
99 northwestern region. Mean annual relative humidity is 30%–40%, with a minimum of less than
100 5%. Modern glaciers have formed in the mountains on the western, southern and northeastern sides
101 of the basin. The basin is surrounded by more than 100 rivers, about 10 rivers of which are
102 perennial, with most of the local rivers being intermittent river systems. The rivers are mainly
103 distributed on the eastern side of the basin but are scarce on the western side. The water in the
104 basin's lakes is predominantly saline, with a total of 31 salt lakes.

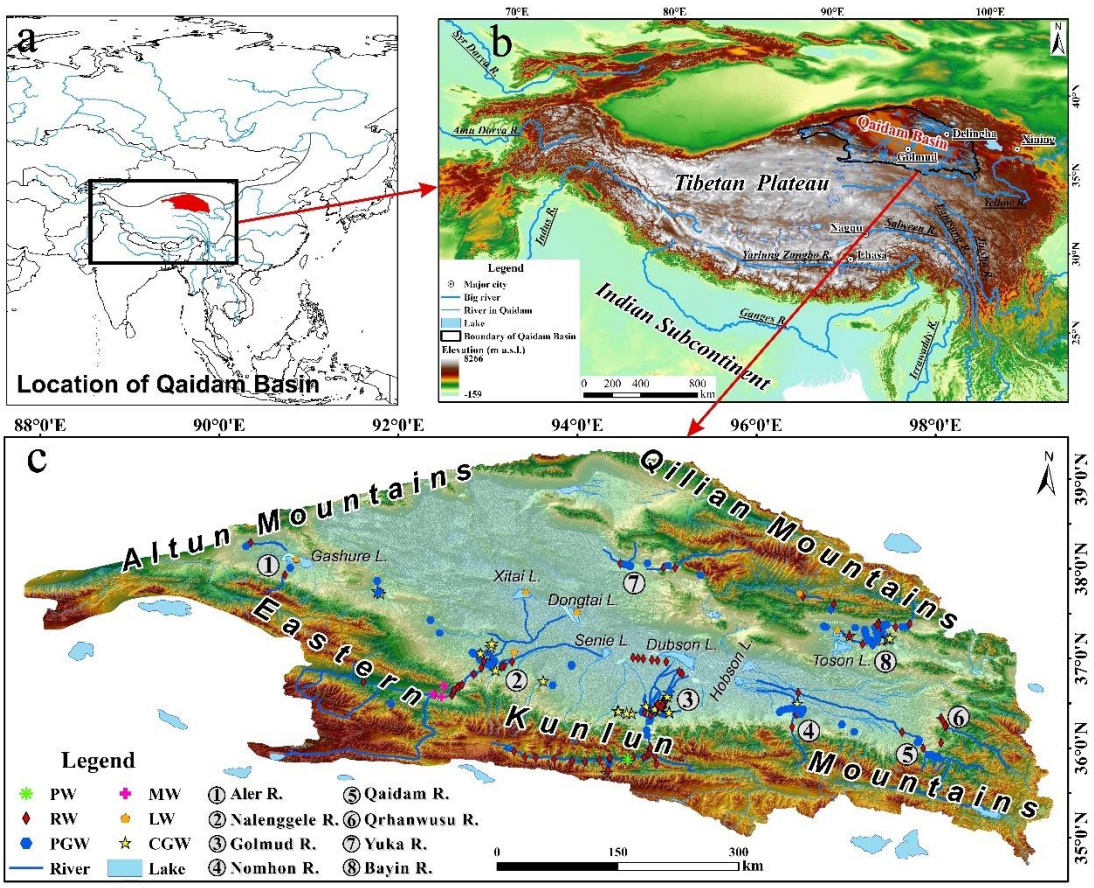


**Figure 1.** Location of Qaidam Basin (a, b) and the sampling sites (c).

## 2.2 Basic hydrogeological setting

The basin basement consists of Precambrian crystalline metamorphic rock series, and the caprock is of Paleogene-Neogene and Quaternary strata. The mountainous area surrounding the basin is dominated by a Paleogene system, and the basin area and basin boundary zone are characterized by a wide distribution of the Paleogene-Neogene system. The Quaternary system is mainly distributed in the central basin region and the intermountain valley region. The basin terrain is slightly tilted from the northwest to southeast, and the height gradually reduces from 3000 m to approximately 2600 m. The distribution of the basin landforms shows a concentric ring shape. From the rim to the centre, the distribution of diluvial gravel fan (Gobi), alluvial–diluvial silt plain, lacustrine–alluvial silt clay plain, and lacustrine silt–salt plains follow a regular pattern. Salt lakes are extensively distributed in the lowlands. The inner edge of the Gobi belt in the northwestern basin region is clustered with hills that are less than 100 m in height. The southeastern region of

the basin has pronounced subsidence, and the alluvial and lacustrine plains are extensive. In the northeastern basin, a secondary small intermountain basin has been formed between the basin and the Qilian Mountains by the uplifting of a series of low mountain fault blocks of metamorphic rock series.

The Qaidam Basin is located in the Qin-Qi-Kun tectonic system, where there is strong neotectonic movement, and a series of syncline-anticline tectonic belts and regional deep faults have formed around it. The fault structures in the Qaidam Basin are very well developed and include the north-easterly Altun fault in the north; north-westerly Saishenteng–Aimunik northern margin deep fault in the northeast; westerly Qaidam northern margin deep fault in the northwest; Qimantag Mountains and Burhan Budai Mountains–Aimunik northern margin deep fault in the south; and north-westerly Sanhu major fault and north-easterly Qigaisu–Dongku Fault in the central basin region.

The distribution of surface water in the basin is constrained by topography and neotectonic movements and appears to have a general centripetal radial pattern (Figure 1c). There is widespread surface water and groundwater exchange. The mountainous areas are rich in precipitation and ice/snow meltwater, and are the main runoff producing areas. Runoff from the mountains flows through the Gobi belt, where most of it infiltrates into the groundwater system. Groundwater discharges to the surface from springs in confined aquifers or springs at the front edge of the alluvial fan. This water finally flows into terminal lakes.

Groundwater can be roughly classified as: i) fractured-bedrock water; ii) leached pore water and local confined groundwater; iii) phreatic groundwater and confined artesian water; iv) saline phreatic groundwater; v) brine, and saline confined artesian water. Surface water and groundwater salinity and solutes are gradually enriched along the flow path (Figure 2; Wang et al., 2008).

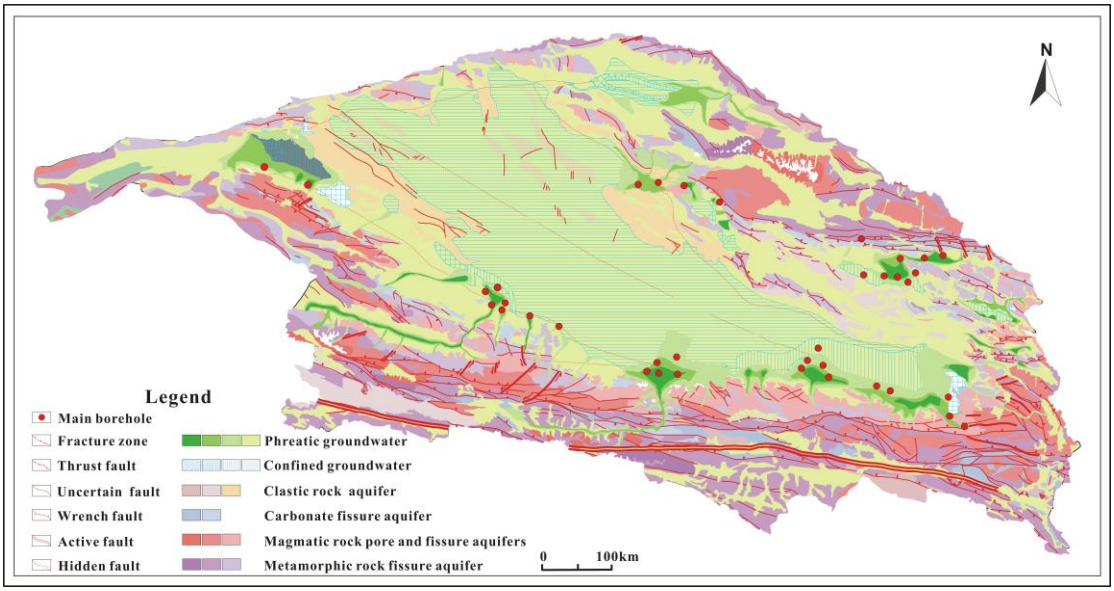


**Figure 2.** Hydrogeologic map of the Qaidam Basin (Modified from Xi'an Center, China Geological Survey, http://www.xian.cgs.gov.cn/). The color of different patches of the same aquifer, from dark to light, denotes high to low in water yield property.

## 3. Sampling and methods

### 3.1 Sampling and analysis

We collected samples from 8 major river–groundwater systems in the region from 2019 to 2021. We collected samples from 6 of the systems once a hydrological year, consisting of the wet season (July–August) and the dry season (March–April). Precipitation and snow meltwater were collected from the Eastern Kunlun Mountains. Snow meltwater was collected in the dry season whereas precipitation was collected at several times during a hydrological year. In total, 239 sampling points were established: phreatic groundwater (n = 100), confined groundwater (n = 43), spring water (n = 6), river water (n = 81), lake water (n = 5), snow meltwater (n = 3), and precipitation (n= 1). A total of 422 sets of samples were collected. No sampling point was established in the northwestern basin because the southern slope and front edge of the Altun Mountains consisted of Tertiary system halite sedimentation and Quaternary system thick salt flats, and no freshwater body was developed. Therefore, the sample collection covers the entire Qaidam Basin and each of the major endorheic regions.

Hydrogen and oxygen isotopes ($^{2}H$, $^{3}H$, and $^{18}O$) were analyzed at the State Key Laboratory of Hydrology-Water Resources and Hydraulic Engineering, Hohai University, China. A MAT253 mass spectrometer was used to measure the ratios of $^{2}H/^{1}H$ and $^{18}O/^{16}O$, and the results were compared with the Vienna Standard Mean Ocean Water (VSMOW), expressed in δ (‰), with the analytical precision (1σ) of the instrument for these isotopes was lower than ±1‰ and ±0.1‰. To determine the tritium ($^{3}H$) concentration, the water sample was first concentrated by electrolysis. Following sample enrichment, measurements were carried out using low background liquid scintillation counting (TRI-CARB 3170 TR/SL). The findings were expressed in terms of absolute concentration in tritium units (TU), the detection limit of the instrument was 0.2 TU, and the precision was improved to less than ± 0.8 TU.

### 3.2 Hydrograph separation

In the analysis of water sources among hydrological processes, endmember mixing models are widely used. The contribution of each recharge endmember to the mixed water body was estimated with a Bayesian mixing model that considers to the heterogeneity of different endmember isotopes/water chemistry parameters (Hooper et al., 1990, 2003; Chang et al., 2018). The process is as follows:

$$1 = \sum_{i=1}^{n} f_i, \quad C_m^j = \sum_{i=1}^{n} f_i C_i^j, j = 1, \dots, n \qquad (1)$$

where $f_i$ represents the proportion of water source $i$, $n$ represents the number of endmembers, and $C_m^j$ represents the level of tracer $j$ in endmember $i$.

The Bayesian mixing models (MixSIAR) coded in R can quantify the contributions of more than two potential endmembers (Parnell et al., 2010). In this study, based on the differences in the water body properties and isotopic composition of each endmember, $\delta^{18}O$, δD, and d-excess (d-excess = $\delta D - 8\delta^{18}O$) data were used as parameters in the modeling. The model was calculated at a fractional increment of 1% and an uncertainty level of 0.1%.

### 3.3 Water vapor trajectory

The source and transport route of moisture can be monitored based on the water vapor flux field derived from the monthly mean ERA5 reanalysis data (0.25° × 0.25°) of the European Centre

for Medium-Range Weather Forecasts (ECMWF, https://www.ecmwf.int/) (Hersbach et al., 2019). After taking into account that more than 70% of the precipitation in the Qaidam Basin occurs from June to September, the monthly mean ERA5 reanalysis data in this period from 2019 to 2021 were used to analyze the water vapor transport path in and around the study area. Based on the average altitude of >3000 m at the study site, the simulated atmospheric pressure was set to 500 hPa. The majority of the atmospheric water vapor was distributed in the range of 0–2 km above ground, and the simulated height did not have any significant influence on the findings (Li and Garzione, 2017; Yang and Wang, 2020).

## 4. Results

### 4.1 Spatial and seasonal characteristics of surface water $\delta^{18}O$-$\delta D$

In the Qaidam Basin, considerable spatial and seasonal variations exist in the stable H-O isotopes of surface water (Figure 3). The isotopic compositions of rivers originating from the Eastern Kunlun Mountains contrast with those from Qilian Mountains, where the heavy isotopes of the Eastern Kunlun Mountains are gradually depleted in the direction of west to east, and the reverse holds true for the Qilian Mountains. Of these, the $\delta^{18}O$ and $\delta D$ values are significantly positive in the southwestern basin, while significantly negative in the eastern basin. Apart from the Nomhon River, all watersheds exhibit a characteristic seasonal variation of enriched in heavy isotope during the wet season relative to the dry season. The mean $\delta^{18}O$ and $\delta D$ values in surface water are more positive by −0.08‰ to 1.08‰ and 0.6‰ to 10.6‰, respectively, in the wet season. Moreover, the seasonal variations of $\delta^{18}O$ and $\delta D$ are more evident in the downstream river compared to the upstream. For instance, the $\delta^{18}O$ value of the downstream Nomhon River is 3.66‰ higher during the wet season compared to the dry season. These phenomena reflect the differences in the recharge sources of the river during both the wet and dry seasons and the strong evaporation effect in the central basin region.

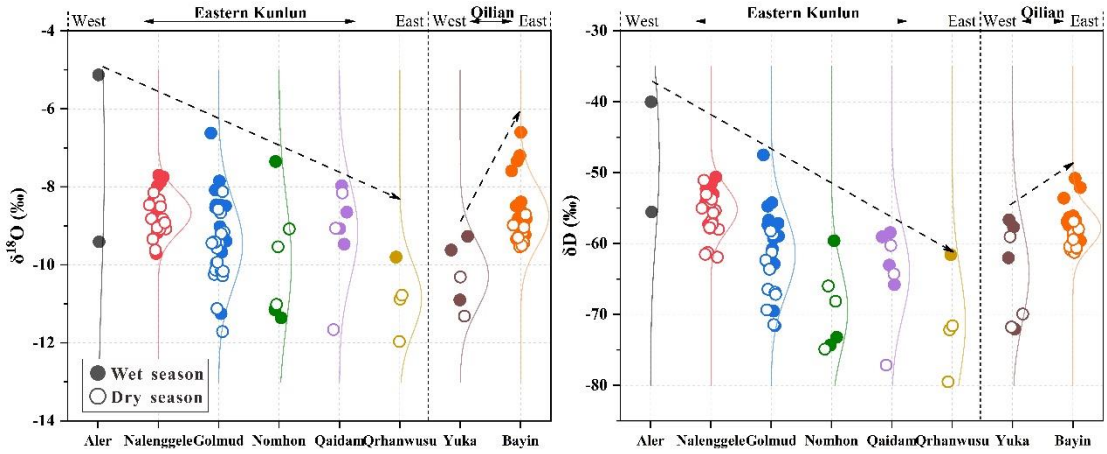


**Figure 3.** Spatial and temporal variation in the H-O isotope composition of Qaidam Basin river water. Filled and hollow dots indicate wet and dry seasons, respectively; The light lines indicate the trend of $\delta^{18}O$ and $\delta D$ from west to east.

## 4.2 Spatial and seasonal characteristics of groundwater $\delta^{18}O$-$\delta D$

The spatial variability of groundwater stable H-O isotopes is more pronounced compared with river water, although it appears to follow the same distribution pattern as river water in the basin (Figure 4). The $\delta^{18}O$ and $\delta D$ values in groundwater system are lower and seasonal fluctuations were smaller compared to those in surface water because the kinetic fractionation of isotopes caused by evaporation and mixing are weaker in groundwater than in surface water. Specifically, the average seasonal variation of $\delta^{18}O$ in each of the groundwater systems ranges from −0.75‰ to +0.84‰, and the largest seasonal variations in individual boreholes are +3.31‰ and −3.16‰, respectively. This suggests that the groundwater reflects a spatial and temporal average of the surface water isotopic signal, and averaging reduces the variability of the values. The region with the greatest seasonal fluctuations of groundwater is located in the Nalenggele River, southwestern basin, and the groundwater $\delta^{18}O$ and $\delta D$ in wet season are noticeably more positive compared to those in dry season. This indicates that groundwater is flowing rapidly and each season, new infiltration displaces the earlier infiltration. The adjacent Golmud River, however, has the least seasonal variations in $\delta^{18}O$ and $\delta D$. In contrast, this suggests that flow is slow. Although there are no obvious differences in the topography and landforms between the two adjacent watersheds, significant differences are observed in the isotope signatures of the two, where both surface water and groundwater show much more positive $\delta^{18}O$ and $\delta D$ values in the Nalenggele River than that of Golmud River catchment.

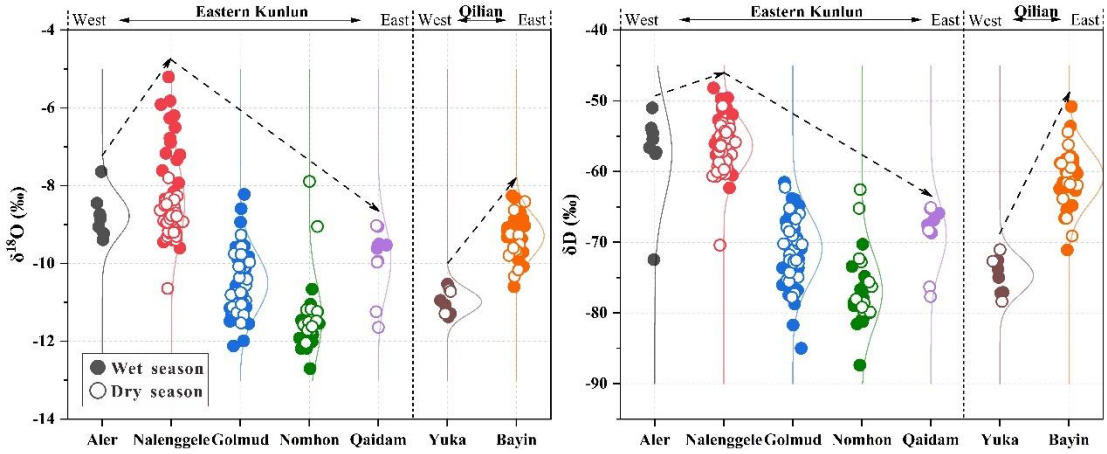


**Figure 4.** Spatial and temporal variation in H-O isotopes in the groundwater of the Qaidam Basin. Filled and hollow dots indicate wet and dry seasons, respectively; The light lines indicate the trend of δ18O and δD from west to east.

## 4.3 Isotopic variations in different water bodies

In the Qaidam Basin, the ranges of $\delta^{18}O$ and δD of the precipitation samples from the Kunlun Mountains and Qilian Mountains are −23.38‰ to +2.55‰ and −158.6‰ to +30.5‰, respectively (Table S1; Zhu et al., 2015). The fitted local meteoric water line (LMWL) equation in the Qaidam Basin is $\delta D = 7.48\delta^{18}O + 11.30$ ($R^2 = 0.95$, n = 74), where the slope and intercept are similar to the long-term monitoring findings of the Qilian Mountains (Figure 5; Zhao et al., 2011; Juan et al., 2020; Wu et al., 2022; Yang et al., 2023). In the Qaidam Basin, the heavy isotopes present in snow meltwater samples are considerably depleted compared to rainwater (Clark and Fritz, 2013). The $\delta^{18}O$ and δD ranges are −19.30‰ to −2.19‰ and −152.0‰ to 32.4‰ respectively, and the fitting trend equation was $\delta D = 9.21\ \delta^{18}O + 31.78$ ($R^2 = 0.89$, n = 12), with the slope and intercept greater than LMWL and GMWL (Global meteoric water line).

The $\delta^{18}O$ and δD ranges in river water are −13.51‰ to −5.93‰ and −85.0‰ to −47.5‰ respectively, whereas those in the lake water are more enriched at −4.10‰ to 8.84‰ and −31.1‰ to 22.1‰, respectively (Figure 5). The fitted trend lines for river and lake samples are: $\delta D = 5.97\delta^{18}O - 5.54$ ($R^2 = 0.85$, n = 92) and $\delta D = 4.64\delta^{18}O - 16.37$ ($R^2 = 0.99$, n = 7), respectively, which are below both the GMWL and LMWL, indicating varying extents of evaporative fractionation in the surface water bodies, with evaporation from lakes being more enhanced. The radioactive $^{3}H$ concentrations range from 4.2 to 17.8 TU, with a mean value of 12.93 TU (n=23, Table S1).

The H-O isotopic composition ranges in the groundwater samples are wider and considerable differences are observed between phreatic and confined groundwater (Figure 5). The $\delta^{18}O$ and $\delta D$ values range in phreatic groundwater from −12.70‰ to −5.21‰ and −87.4‰ to −42.0‰, respectively. The fitted trend line is $\delta D = 5.73\delta^{18}O - 9.20$ ($R^2 = 0.83$, n = 185). The phreatic groundwater isotopic composition and slope of the trend line are similar to those of surface water, indicating considerable interactions between the two and substantial evaporative fractionation of some shallow groundwater. The $\delta^{18}O$ and $\delta D$ ranges in confined groundwater are relatively small and lower in comparison at −12.12‰ to −8.58‰ and −85.0‰ to −51.0‰. The linear regression relationship of the samples fitting ($\delta D = 7.84\delta\ ^{18}O + 12.39$, $R^2 = 0.87$, n = 51) revealed that its slope and intercept were essentially consistent with those of GMWL and LMWL, suggesting the presence of a strong correlation between confined groundwater and atmospheric precipitation in different periods. Radioactive $^{3}H$ concentrations detectable in the phreatic and confined groundwater range from 0.22 to 30.35 TU and 0.60 to 12.76 TU, respectively, with mean values of 10.23 TU (n=49) and 7.55 TU (n=10), respectively (Table S1).

Overall, the stable H-O isotopic compositions of surface water and groundwater are generally more enriched in the Qaidam Basin. The isotopic compositions and trend fitting features both demonstrated that the water samples have undergone varying degrees of evaporation during runoff, indicating the cold and dry climate environmental characteristics of the study area.

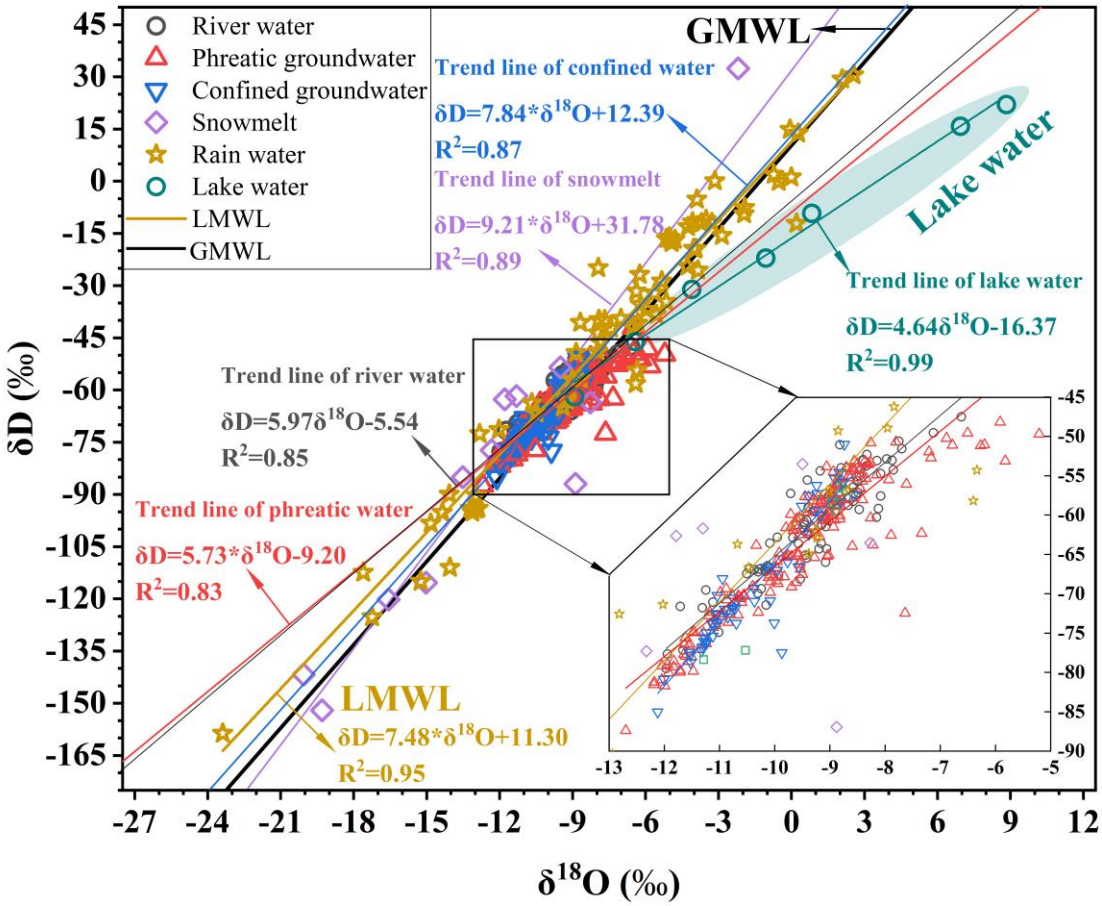


**Figure 5.** Plot of the relationships between $\delta^{18}O$ and $\delta D$ in different water bodies from the Qaidam Basin.

## 5. Discussion

### 5.1 Water cycle information indicated by surface water isotopes

#### 5.1.1 Atmospheric moisture transport pattern

To further explain the cause of spatial and seasonal variations of surface water $\delta^{18}O$ and $\delta D$ values, ERA5 reanalysis data in the rainy season (June to September) were used to calculate the water vapor flux field in the Qaidam Basin and its surrounding areas as well as track the main trajectories of the moisture transport (Hersbach et al., 2019). The results show that the mid-latitude westerlies dominate the moisture paths inside and around the basin, and the water vapor flux in the eastern basin is notably greater than that in the western basin (Figure 6; Yang and Wang, 2020). This largely explains the spatial patterns of river water H-O isotopes (Figure 3), as well as temperature and precipitation regimes (Figure S1). Atmospheric and isotopic tracing data also support these conclusions. For instance, the Tanggula Mountains (33°–35° N) serve as the physical

and chemical boundary of the Tibetan Plateau, and the westerlies fundamentally govern the northern region, preventing the Indian monsoon from having a significant impact on the Qaidam Basin (Yao et al., 2013; Kang et al. 2019; Wang et al., 2019). Furthermore, d-excess can effectively represent the moisture source properties. The mean d-excess of basin river water during the wet season (11.45‰, Table S1) was greater than 10‰, associated with the characteristics of an alpine arid continental climate and a moisture source devoid of monsoon influences. Higher d-excess values are attributed to westerlies moisture and recycled moisture that is boosted by inland surface evaporation. In contrast, the hinterland of the Tibetan Plateau, south of the Tanggula Mountains, which was subject to significant influences from the Indian monsoon circulation, had summer precipitation and river water d-excess values that ranged from 5‰ to 9‰ with a mean value of 7‰ (Tian et al., 2001). The stark contrasts in the d-excess values between the two regions further support the above inference about the moisture sources of the Qaidam Basin.

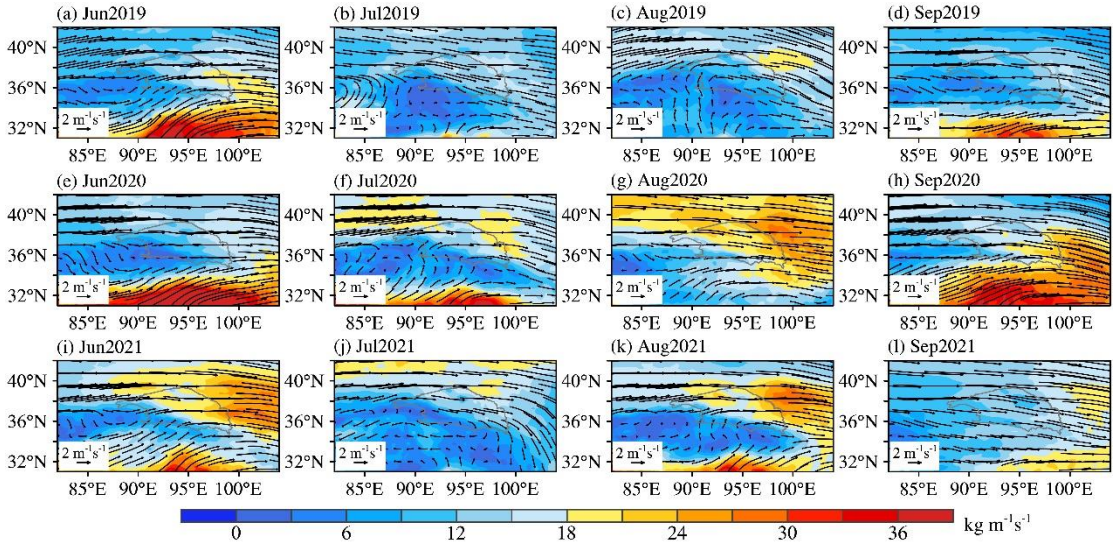


**Figure 6.** Tropospheric water vapor flux from June to September 2019 to 2021 (below 500 hPa, unit: kg $m^{-1}s^{-1}$).

### 5.1.2 Isotopic records of surface water to precipitation

Owing to the sparse precipitation in the alpine arid region and its concentration in summer (June to September), surface water isotopic records may mimic local precipitation characteristics during the wet season. On a seasonal basis, the positive correlations between isotopic variations in surface water (Figure 3) and those in precipitation are extremely strong across most of the basin and its surrounding areas (Liu et al., 2009; Zhao et al., 2011; Juan et al., 2020; Wu et al., 2022). In particular, the $\delta^{18}O$ values in the mountainous areas of each watershed are higher during wet season

compared to the dry season, reflecting the input of precipitation with heavy isotopic signatures to the river. Moreover, the mean $\delta^{18}O$ and $\delta D$ values are higher in watersheds (such as Qaidam and Bayin Rivers) during wet season, with correspondingly excessive rainfall (Figure S1). From this, river water isotopes of each watershed in the basin are primarily impacted by summer precipitation during the wet season could be inferred. This is mostly because during the rainy season, relatively intensive rainfall events can create surface runoff and rapidly recharge the river.

5.1.3 Climate impact on isotopic spatial and temporal variation

The spatial variation of surface water isotopes of the Eastern Kunlun Mountains water system (Figure 3) reflects the variation of precipitation isotopes which are strongly influenced by westerlies moisture transport. Heavy isotopes are preferentially separated in raindrops condensation along the westerlies trajectory, and long distance moisture advection leads to heavy isotope depleted precipitation due to rainout (Wang et al., 2016; Yang and Wang, 2020). Meanwhile, the isotope variations in the two watersheds in the Qilian Mountains are opposite to those in the Eastern Kunlun Mountains. Comparing the meteorological parameters of Delingha and Da Qaidam (refer to Figure S1 for specific location) from 2010 to 2020, the mean annual precipitation of Delingha (276.36 mm) was 2.41 times higher than that of Da Qaidam (114.79 mm), and the mean annual temperature of Delingha (5.23 °C) was 1.58 °C higher than that of Da Qaidam (3.65 °C). Precipitation in the Bayin River has increased by up to 25.09 mm per decade since 1961 (Figure S1). The seasonal $\delta^{18}O$ variation in the Bayin River is roughly 1.79 times that of the Yuka River, due to the marked increase in precipitation in Delingha. Under similar conditions of ice/snow meltwater recharge, the mean $\delta^{18}O$ and $\delta D$ values of the Bayin River are higher than 1.52‰ and 7.3‰, respectively, relative to that of the Yuka River, which can be attributed to a greater proportional contribution of precipitation with heavy isotopic signatures. As a result, the change in river water isotopes in the Qilian Mountains can be attributed to the differences in temperature and precipitation regimes, as well as the extents of warming and humidification between the watersheds.

Given the spatial and temporal variations of surface water $\delta^{18}O$-$\delta D$ (Figure 3), samples from different water bodies within each watershed were incorporated into the $\delta^{18}O$-$\delta D$ plot (Figure 7). The considerable differences in the dual-isotopic spectrum imply that seasonal variations in surface water isotopes in each watershed may be attributed to variability in the contribution ratios

of precipitation, ice/snow meltwater, and groundwater throughout both the wet and dry seasons. Hence, Equation 1 of the MixSIAR model was employed to estimate the contribution of each potential recharge endmember to river water (Table 1). The findings reveal that groundwater discharge in mountainous areas maintains the base flow in each watershed during dry season, with groundwater contribution up to 97% of the total flow. Various proportions of precipitation, ice/snow meltwater and groundwater recharge the river water during the wet season. For example, in the area with the greatest annual precipitation, the contribution of summer precipitation to the Bayin River during the wet season may reach 84%. Thus, variability in the proportional contributions of each recharge endmember during wet and dry seasons are the main factors responsible for the seasonal variations in surface water isotopes in each watershed.

In summary, the spatial and seasonal variations of surface water stable isotopes are caused by the interaction of regional warming and humidification trends, the intensity of midlatitude westerlies moisture transport, and local hydrometeorological conditions.

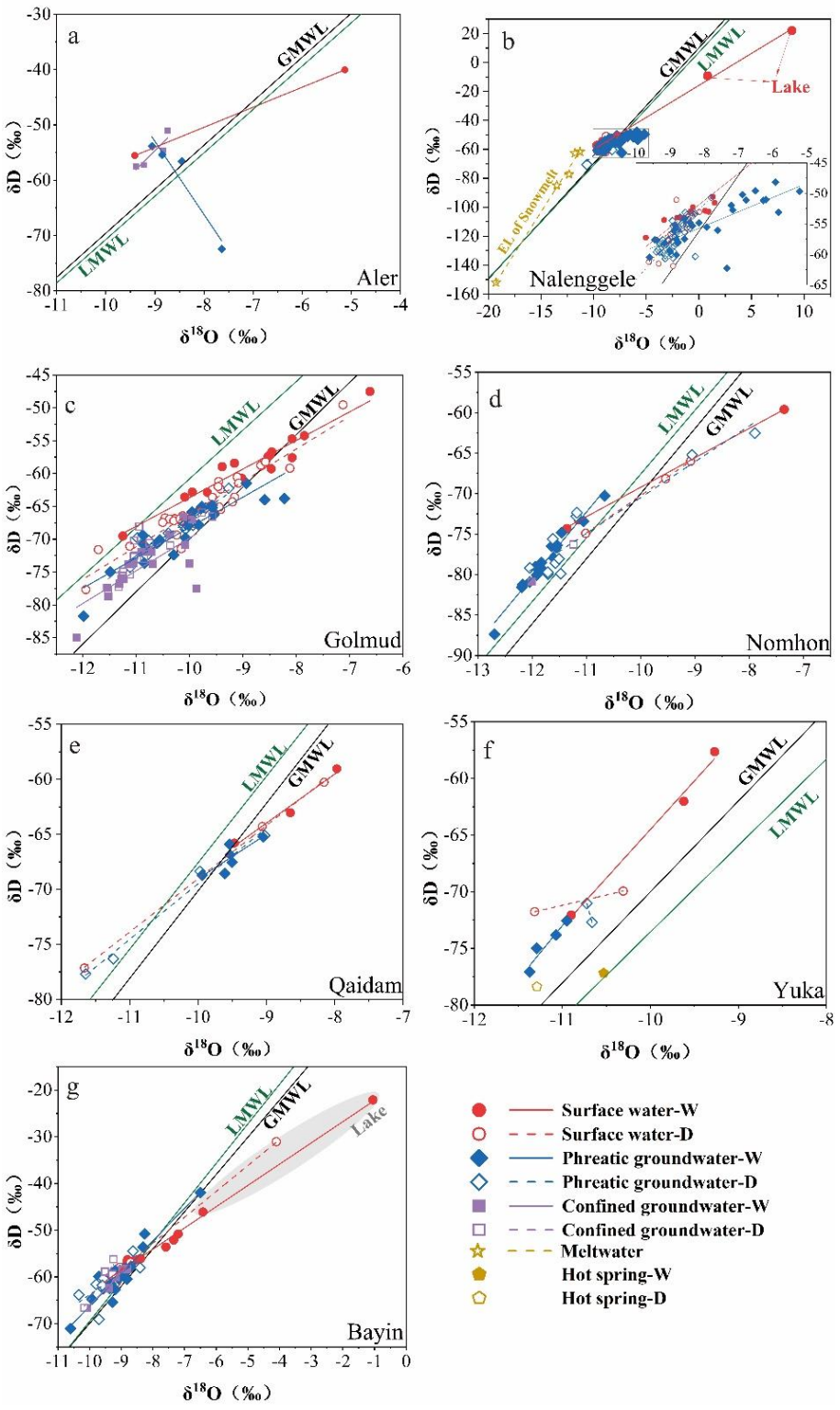


353

354 **Figure 7.** $\delta^{18}O$-$\delta D$ plots in different water bodies in each watershed of the Qaidam Basin during dry and wet
355 seasons. W and D represent wet and dry seasons, respectively. Data source of LMWLs: a and b: Xu et al., 2017;
356 c: this study; d and e: Xiao et al., 2017; f: Zhu et al., 2015; g: Tian et al., 2001.

**Table 1.** Contribution ratios of endmembers to river water during the wet and dry seasons based on δ18O and d-excess (Unit: %; W and D represent wet and dry seasons, respectively).

| | Endmember | Groundwater | Meltwater | Tributary | Precipitation |
|---|---|---|---|---|---|
| Nalengele-W | Mean | 0.41 | | 0.47 | 0.12 |
| | Max | 0.60 | | 0.74 | 0.13 |
| | Min | 0.18 | | 0.27 | 0.08 |
| | SD | 0.12 | | 0.13 | 0.02 |
| Nalengele-D | Mean | 0.90 | 0.10 | | |
| | Max | 0.97 | 0.27 | | |
| | Min | 0.73 | 0.03 | | |
| | SD | 0.07 | 0.07 | | |
| Golmud-W | Mean | 0.31 | 0.34 | 0.25 | 0.10 |
| | Max | 0.36 | 0.39 | 0.32 | 0.12 |
| | Min | 0.28 | 0.29 | 0.20 | 0.08 |
| | SD | 0.03 | 0.04 | 0.05 | 0.01 |
| Golmud-D | Mean | 0.32 | 0.25 | 0.42 | |
| | Max | 0.46 | 0.45 | 0.70 | |
| | Min | 0.19 | 0.11 | 0.21 | |
| | SD | 0.09 | 0.10 | 0.17 | |
| Yuka-W | Mean | 0.62 | 0.23 | | 0.15 |
| | Max | 0.76 | 0.29 | | 0.18 |
| | Min | 0.55 | 0.15 | | 0.10 |
| | SD | 0.10 | 0.06 | | 0.04 |
| Bayin-W | Mean | 0.26 | 0.04 | 0.25 | 0.45 |
| | Max | 0.35 | 0.05 | 0.43 | 0.84 |
| | Min | 0.08 | 0.02 | 0.06 | 0.23 |
| | SD | 0.08 | 0.01 | 0.11 | 0.19 |

## 5.2 Multi-sources of groundwater recharge and circulation mechanism

Seasonal variations in groundwater aquifer H-O isotopes in each watershed suggest that their recharge sources, forms, and rates fluctuate. The $\delta^{18}O$-$\delta D$ correlations of different seasons and types of water samples can be used to deduce the groundwater source compositions and recharge patterns. According to the seasonal variations in groundwater $\delta^{18}O$-$\delta D$ in each watershed (Figure 4) and the dual-isotopic spectrum of different water bodies within the watershed (Figure 7), the Qaidam Basin groundwater systems can be divided into three recharge types: modern precipitation and glacier snow melt water dominated recharge and fossil water as well.

### 5.2.1 Precipitation dominated recharge

In the Nalenggele River, which is situated in the southwestern basin, and the Qaidam and Bayin Rivers in the eastern basin, groundwater $\delta^{18}O$ and $\delta D$ values are markedly positive in wet season and negative in dry season (Figure 5). The groundwater isotope data in the majority of the wet season clusters near the LMWL and GMWL compared to that during the dry season (Figures 7b, 7e, and 7g), indicating the isotopic signatures are similar to the river water and summer precipitation in the same period (Table S1; Zhu et al., 2015), with different trends in evaporation. These results suggest precipitation recharges groundwater during the wet season. The significant seasonal variations of H-O isotopes show that the aquifers in the eastern and southwestern Qaidam Basin have relatively rapid groundwater circulation and seasonal recharge. There is an abundance and notable rise in precipitation in the eastern basin (Figure S1). An interesting finding was that increased precipitation has directly caused a rise of 5 m in water level and an area expansion of 1.59 times in a lake near the headwaters of the Nalenggele River in the southwestern basin from 1995 to 2015 (Chen et al., 2019). The abundant Precipitation observed in the eastern basin headwater may also be a potential source for the rapid seasonal groundwater recharge associated with rapid warming and humidification. Furthermore, the tectonic conditions of the recharge area are believed to enhance seasonal groundwater recharge. The three watersheds coincide with collision zones of intensive neotectonic movement, where a considerable number of deep faults and other volcanic channels have developed within recharge areas (Figure 2; Tan et al., 2021). It can be concluded that favorable hydrological and tectonic conditions facilitate the formation of directly rapid groundwater recharge of precipitation and meltwater through bedrock fissures at high altitudes under large hydraulic heads (>1000 m), resulting in significant seasonal variations in the groundwater H-O isotopes in these regions.

### 5.2.2 Glacier snow melt water dominated recharge

In the Nomhon and Yuka Rivers, located in the middle region of the basin, groundwater H-O isotopes are more depleted in the wet season than in the dry season (Table S1; Figure 4). Most of the $\delta^{18}O$–$\delta D$ data for the groundwater samples in these two watersheds are observed in the lower left of the LMWL and GMWL (Figures 7d and 7f), and these values are more negative relative to river water, with characteristics parallel to those measured in snowmelt water obtained from the high-altitude Eastern Kunlun Mountain (Figure 5; Yang et al., 2016). This shows that the

groundwater recharged by ice/snow meltwater is more isotopically depleted during both the wet and dry seasons, despite the fact that precipitation contributes less to the aquifer. Similarly, non-monsoonal meltwater control of hydrological processes in monsoonal groundwater systems has also been observed on the eastern margin of the Tibetan Plateau (Kong et al., 2019). The isotope signals suggested that isotopically depleted ice/snow meltwater in the source region was released due to elevated summer temperatures, and was further depleted in the groundwater after mixing with groundwater recharged by seasonal meltwater. Furthermore, due to the scarce precipitation in these two watersheds (61.39 and 121.78 mm, respectively, Figure S1), and that even fewer precipitation events occurred in 2020, the seasonal direct recharge to the aquifer from the limited precipitation was negligible in this extremely arid climate.

### 5.2.3 Fossil water dominated recharge

In the Golmud River, the mean $\delta^{18}O$ value is 0.33‰ higher during the wet season than during the dry season, with insignificant seasonal changes, indicating a limited share of seasonal groundwater recharge and a slow renewal rate. The groundwater H-O isotope data lay mainly between the LMWL and GMWL (Figure 7c), implying that the predominant recharge source is different periods atmospheric precipitation (Beyerle et al., 1998). Furthermore, the groundwater $\delta^{18}O$ and $\delta D$ values exhibit a gradually decreased trend along the flow path (Figures 8a and 8b). For this watershed, a prominent feature is the sizeable storage of confined groundwater, which is constantly discharging at the front edge of the alluvial fan. Confined groundwater $\delta^{18}O$ and $\delta D$ values are more negative than those of phreatic groundwater, and the mean $\delta^{18}O$ values are similar during the wet and dry seasons, with minor seasonal variation (Table S1). We hypothesize that phreatic groundwater is recharged primarily by ice/snow meltwater, while confined groundwater is slowly and stably recharged and may be sustained by precipitation with low $\delta^{18}O$ and $\delta D$ values or fossil water formed during relatively cold climate periods (Xiao et al., 2018). This scenario is in fact observed in deep confined groundwater in many areas in the world (Ma et al., 2009; Jasechko et al., 2017).

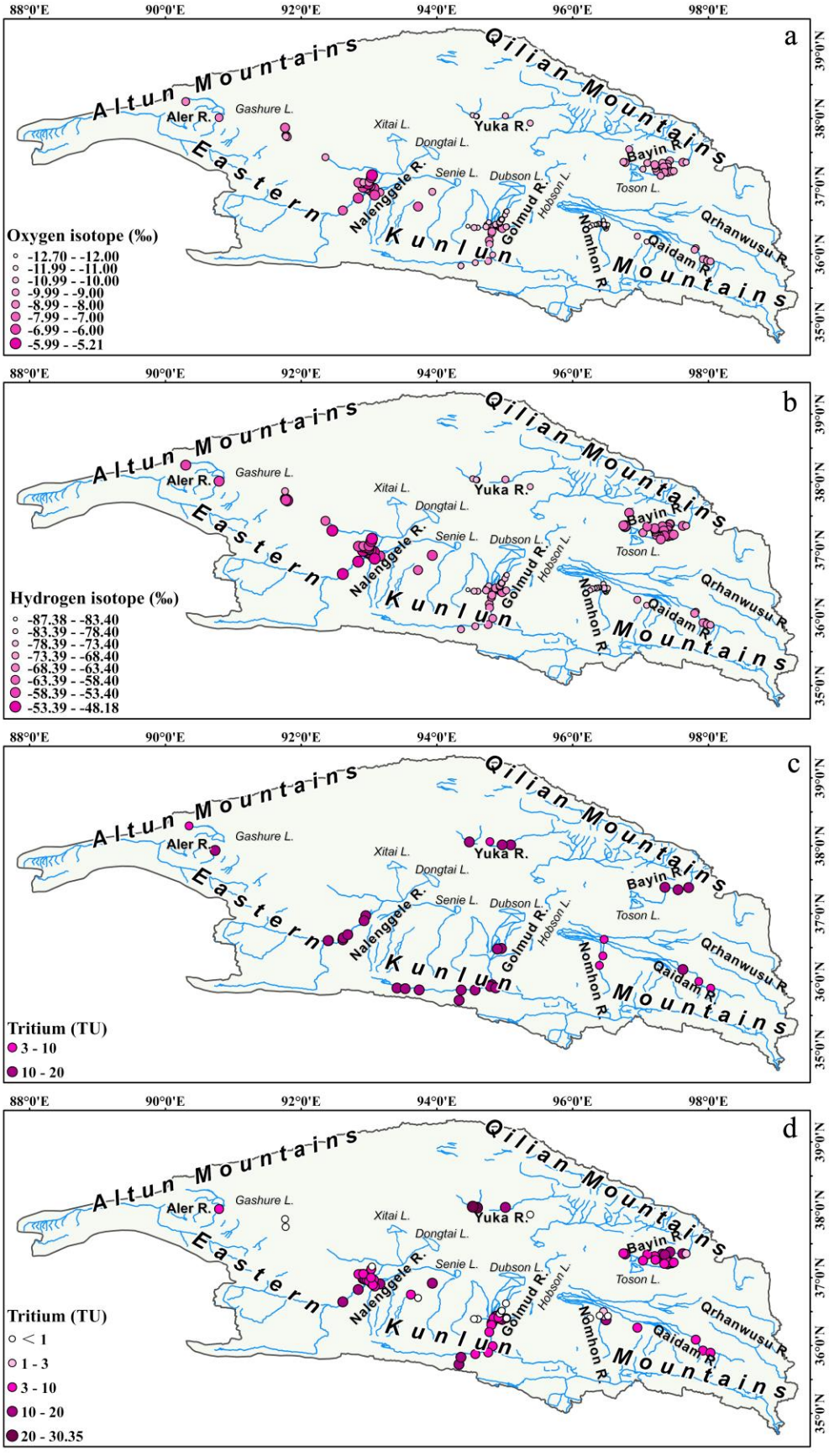
a
Altun Mountains
Qilian Mountains
Eastern Kunlun
Mountains
Aler R.
Gashure L.
Xitai L.
Yuka R.
Dongtai L.
Bayin R.
Toson L.
Senie L.
Dubson L.
Nalenggele R.
Golmud R.
Hobson L.
Nomhon R.
Qaidam R.
Qrhanwusu R.
Oxygen isotope (‰)
-12.70 - -12.00
-11.99 - -11.00
-10.99 - -10.00
-9.99 - -9.00
-8.99 - -8.00
-7.99 - -7.00
-6.99 - -6.00
-5.99 - -5.21
b
Hydrogen isotope (‰)
-87.38 - -83.40
-83.39 - -78.40
-78.39 - -73.40
-73.39 - -68.40
-68.39 - -63.40
-63.39 - -58.40
-58.39 - -53.40
-53.39 - -48.18
c
Tritium (TU)
3 - 10
10 - 20
d
Tritium (TU)
< 1
1 - 3
3 - 10
10 - 20
20 - 30.35
88°0'E
90°0'E
92°0'E
94°0'E
96°0'E
98°0'E
39°0'N
38°0'N
37°0'N
36°0'N
35°0'N

423

**Figure 8.** Spatial distribution of $\delta^{18}O$ (a) and $\delta D$ (b) in groundwater and tritium concentrations in surface water (c) and groundwater (d) during the wet season.

### 5.2.4 Mechanism governing water cycle in alpine mountain-basin system

Radioactive $^{3}H$, tritium, with a half-life of 12.32 years, can be used to estimate the migration time of younger water. Particularly in mixed water bodies consisting of younger water and fossil water, $^{3}H$ can be used to effectively characterize groundwater age and renewal rate (Stewart et al., 2017; Xiao et al., 2018; Chatterjee et al., 2019; Shi et al., 2021). In accordance with the significant differences in $\delta^{18}O$-$\delta D$ of the various water bodies in each watershed (Figures 7, 8a, and 8b), the scale of the groundwater recharge in the Qaidam Basin is further constrained with $^{3}H$ (Figures 8c and 8d). The spatial pattern of $^{3}H$ reveals that groundwater recharge rates varied significantly at both intra- and inter-watershed scales (Figures 8c and 8d). Thus, the groundwater system is dominated by both regional and local recharge.

At the watershed scale, the $^{3}H$ concentration of phreatic groundwater is significantly higher in alluvial fan areas along the river channel and mountain pass (Table S1; Figures 8c and 8d), and approximates that of the river water. This suggests that there is a close hydraulic connection between surface water and groundwater, and that the aquifer also receives river water through vertical infiltration and lateral recharge. This portion of groundwater is therefore mostly seasonal, younger, and has a rather rapid renewal rate. $^{3}H$ concentrations in the periphery of phreatic and confined groundwater are typically less than 3 TU, indicating that $^{3}H$ is dead in comparison to that near the river channel. These findings suggest that these aquifers are mostly recharged by lateral flow, consisting primarily of sub−modern water (>60 years) or fossil water, with limited mixing of modern precipitation and seasonal meltwater, and a slow renewal rate. This is especially evident in Golmud and Nomhon Rivers (Liu et al., 2014; Cui et al., 2015; Xiao et al., 2017, 2018), highlighting the importance of fossil water content in recharging the aquifer in extremely arid regions.

At the basin scale, $^{3}H$ data is consistent with seasonal variations in stable H-O isotopes. Seasonal variations in $\delta^{18}O$ and $\delta D$ values correspond to higher average $^{3}H$ concentration in phreatic groundwater systems in the eastern and southwestern basin, revealing that seasonal groundwater recharge is more significant, and that groundwater age is overall younger (<60 years). Based on river seepage, modern meltwater and precipitation may potentially infiltrate through

preferential flow paths, such as fault zones developed on a large scale in the recharge area, resulting in rapid aquifer recharge (Figure 9b; Tan et al., 2021). The contrary was observed in the phreatic groundwater systems of the western Qilian Mountains and middle Eastern Kunlun Mountains, where the depletion in heavy isotopes during wet season, accompanied by low $^{3}H$ concentrations, meant these aquifers were primarily recharged by seasonal ice/snow meltwater. In contrast, the groundwater renewal rate was relatively slow, owing to less and more steady meltwater recharge (Figure 9c).

In confined groundwater, heavy H-O isotope depletion is greatest, with most samples having very low $^{3}H$ concentrations (<3 TU), indicating a very slow recharge rate. Furthermore, most of the confined groundwater was over 100 years old and consisted mainly of submodern groundwater or fossil water (Xiao et al., 2018). In the Golmud River, the confined groundwater in the discharge zone continued to discharge after nearly a half century of extraction, and the pressure heads did not decrease, implying that modern precipitation or ice/snow meltwater may recharge deep confined groundwater. Some confined groundwaters possess discernible seasonal isotopic effects, and the existence of a certain proportion of ongoing recharge, even on a seasonal scale, cannot be excluded. Large karst springs have also developed in the mountainous areas of Golmud River. Well-formed karst caves and fissures provide conduits for direct precipitation or meltwater infiltration. With deep circulation, precipitation and meltwater generate regional subsurface flow that recharges the confined groundwater in the overflow zone in the long term, allowing continuous flow under a large hydraulic head (about 1,000 m) (Figure 9d). Moreover, the H-O isotopic signals of confined groundwater in part of the alluvial fan front in the Golmud and Bayin Rivers are largely similar with those of the nearby phreatic groundwater, with $^{3}H$ concentrations close to 10 TU. These findings also suggest that confined groundwater recharge may have occurred through aquitard or by leakage recharge in nearby skylights.

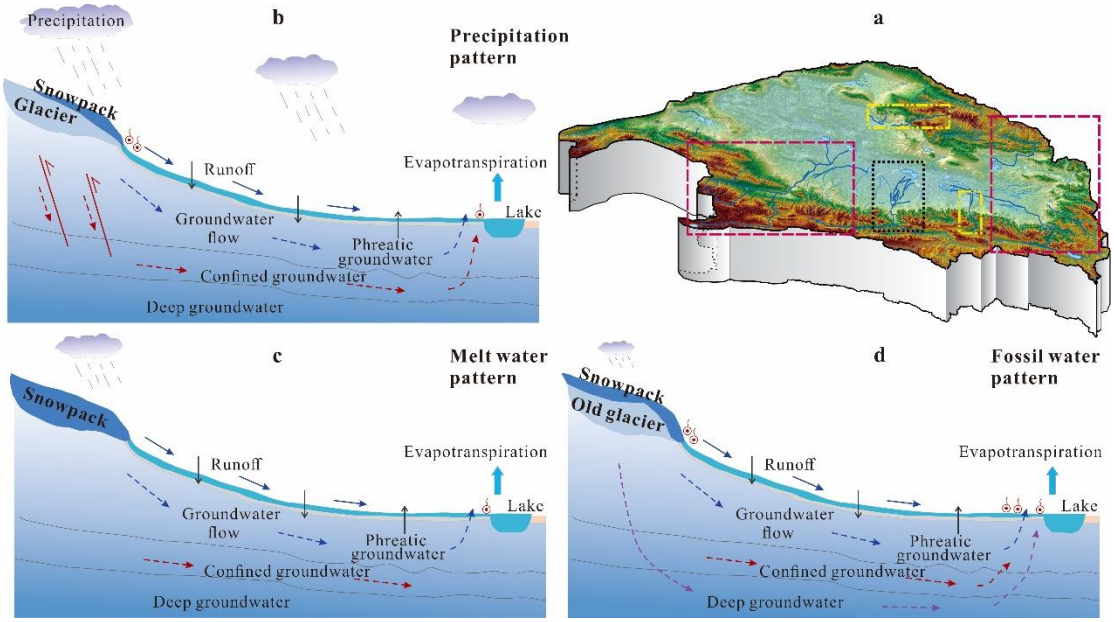


**Figure 9.** Schematic diagram of the Qaidam Basin water cycle model (b represents the purple dashed box; c represents the yellow dashed box; and d represents the black dashed box).

## 5.3 Isotope hydrology responses to climate change and indication of water cycle trends

The Qaidam Basin has experienced rapid warming at a rate more than twice the global average since the 1980s (Wang et al., 2014; Kuang and Jiao, 2016; Yao et al., 2022). Since 1961, the 10- and 30-year mean temperature and precipitation changes and rising rates at eight meteorological stations in the basin have demonstrated that the current warming and humidification trends in this basin, northeastern Tibetan Plateau, are continuously strengthening (Figure 10). Changes in surface water and groundwater isotopes in the Qaidam Basin reflect different sensitivities to climate change at both seasonal and multi-year scales. Previously, it was assumed that the isotopic composition of the surface water and groundwater systems did not vary with time, at least on interannual intervals, and was rather stable (Boutt et al., 2019). However, isotopic variability in water bodies over the past 40 years suggests that there is a variable degree of interannual variability in surface water and groundwater isotopes, with interannual variability in mean $\delta^{18}O$ values greater than 3‰ (Figure 11). The spatial and temporal variability of isotopic signals can be ascribed to differences in the extent of warming and humidification across the basins. Wang et al. (2014) highlighted that while the Qaidam Basin has experienced rapid warming over the past 50 years, warming and humidification have been markedly asynchronous in different regions, with rates of temperature increase ranging from 0.31 to 0.89 ℃ per decade and the rates

of rainfall increase from 1.77 to 25.09 mm per decade (Figure S1). It is noteworthy that surface water is more responsive to precipitation, whereas groundwater is more sensitive to temperature (Figure 12). This phenomenon suggests that increased precipitation may influence the water cycle by promoting slope runoff and groundwater infiltration in mountainous areas, and the warming will cause the solid water ablation at higher elevations, thereby accelerating groundwater recharge to aquifers through bedrock fissures. In addition, elegant remote sensing monitoring findings suggested that the increase in terrestrial water storage in the Qaidam Basin was strongly correlated with increased precipitation and glacier meltwater recharge (Song et al., 2014; Jiao et al., 2015; Xiang et al., 2016; Wei et al., 2021; Zou et al., 2022), which fully supported the isotope-based conjecture. Furthermore, a recent study found that the accelerated conversion of ice and snow into liquid water on the Tibetan Plateau has led to an imbalance in the "Asia Water Tower", with the Qaidam Basin being one of the key regions where liquid water has grown (Yao et al., 2022). The isotopes, remote sensing and hydrometeorology data are consistent with the observation that the Qaidam Basin is the most rapid and substantial warming region in the Tibetan Plateau. Global warming affects the basin by redistributing precipitation and melting ice and snow in high elevations, resulting in groundwater storage increase and lakes expansion. The trend of increasing water storage in the Qaidam Basin is likely to continue in the 21st century. The highly coupled results of different observation methods further emphasize the sensitivity and potential of water isotopes in tracing water cycles and climate change.

Under the influence of climate change and the intensive cryosphere retreat, runoff has changed dramatically on the Tibetan Plateau, with significant effects on the spatial and temporal water resources distribution (Wang et al., 2021). The rapid changes in water resources in the Qaidam Basin are likely because:

1) The surface water and groundwater resources will increase significantly in the short term (in recent decades) due to continued rapid warming and wetting. For example, water storage in the Bayin and Qaidam Rivers in the eastern basin is likely to continue to increase with a high renewal capacity in the long term under the influence of sustained climate change and the abundant and significantly increasing precipitation. This phenomenon has been verified in many regions of the Tibetan Plateau as well as some alpine watersheds in high-latitude Switzerland (Xiang et al., 2016; Malard et al., 2016; Shi et al., 2021).

2) The decadal scale climatic oscillation suggests that the massive shrinking cryosphere may not sustain surface water and groundwater recharge in the basin (Wang et al., 2023). It is expected that water resources in the southwestern basin (e.g., Nalenggele River) may continue to increase for a certain period followed by a large-scale decrease under future climate change scenarios. This is a general trend that has occurred in the Tibetan Plateau as well as regions around the world with large-scale glacial coverage area in alpine watersheds. Glaciers in the southwestern basin are reported to be losing mass regularly (−0.2 to −0.5 m/a), a trend that has increased substantially from 2018 to 2020, notably at the headwaters of Nalenggele River, where glacier elevation has been reduced by 5.42 m since 2000 (Shen et al., 2022). However, completing the hydrologic budget will remain a challenge given strong decoupling between rapid melting of ice and snow caused by warming versus scarce precipitation in the southwestern basin, even if precipitation continuously increases in the future.

3) In the middle basin (Nomhon, Golmud, and Yuka Rivers), there is long-term large-scale groundwater mining during the agriculture and industry development, accompanied by strong local evaporation. The sparse precipitation in the source area led to a melt dependence, although the surface water and groundwater recharge here are relatively stable.

4) Future groundwater level dropping seems to be inevitable in the basin with glacier retreat and reducing of melt water in the mountainous source area. Monitoring data from five shallow groundwater boreholes along the alluvial fan belt of the Golmud River shows that groundwater levels have fluctuated since 2011, declining by an average of −1.18 m/a (Figure S2). Therefore, whether the enhanced water resource renewal capacity and water storage in the Qaidam Basin can stay stable in the future is a scientific issue worth considering.

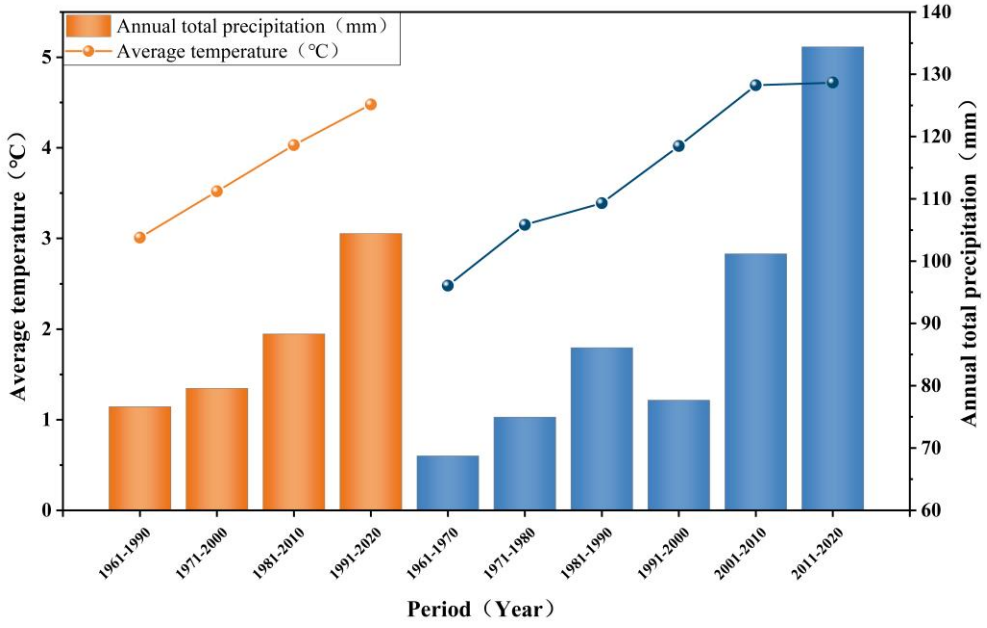


552

553 **Figure 10.** Average temperature and precipitation in the Qaidam Basin every 30 years and 10 years from 1961
554 to 2020.

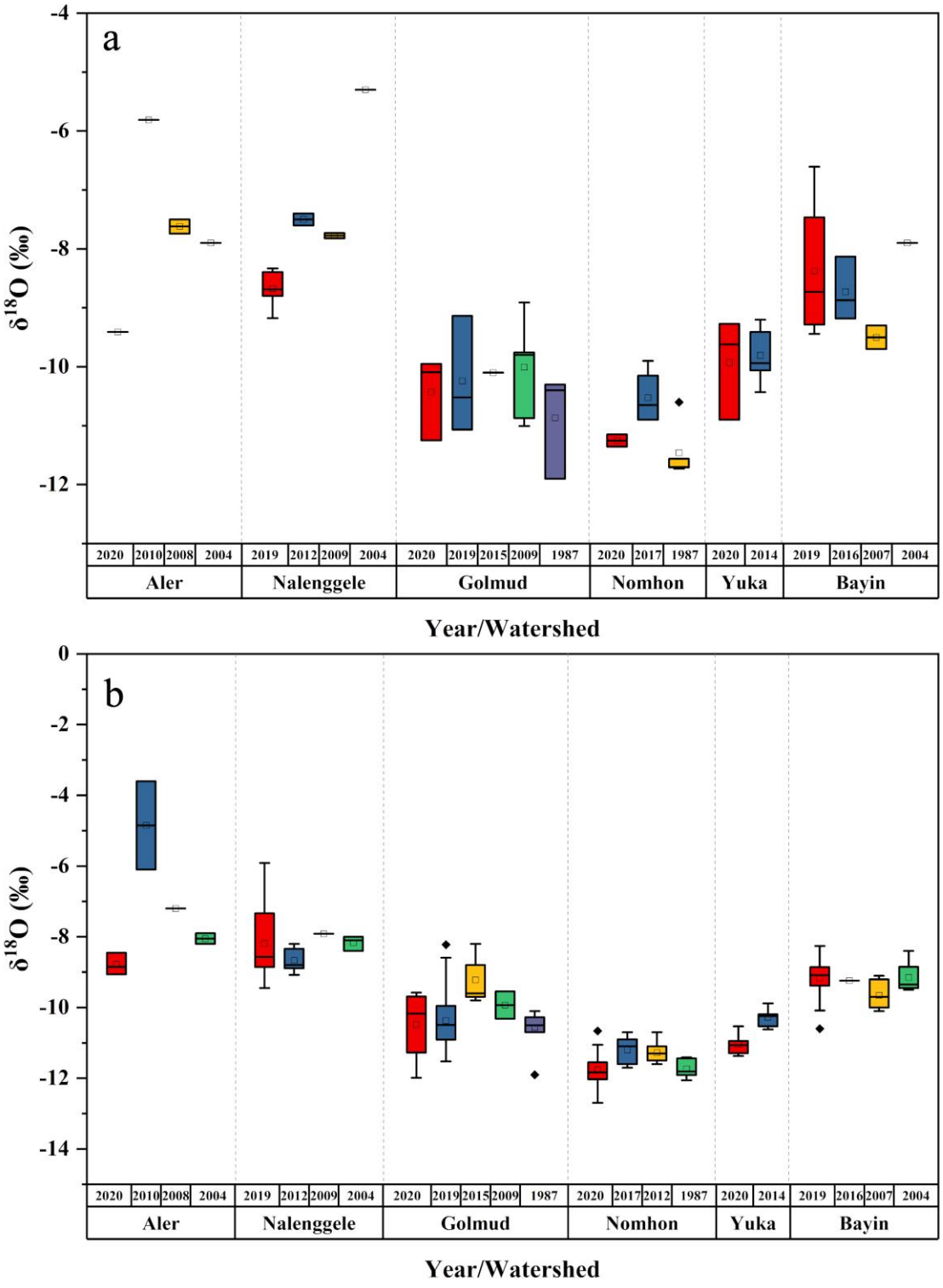


555

556 **Figure 11.** Interannual variations in the river water (a) and groundwater (b) $\delta^{18}O$ in the Qaidam Basin. Date
557 source: Aler: 2004, Wang et al., 2008; 2008, Tan et al., 2009; 2010, Ye et al., 2015. Nalenggele: 2004,
558 Wang et al., 2008; 2009, Tan et al., 2012; 2012, Xu et al., 2017. Golmud: 1987, Wang et al., 2008; 2009,

559 Tan et al., 2012; 2015, Xiao et al., 2018. Nomhon: 1987, Wang et al., 2008; 2012, Cui et al., 2015; 2017,
560 Zhao et al., 2018. Yuka: 2014, Zhu, 2015. Bayin: 2004, Wang et al., 2008; 2007, He et al., 2016; 2016,
561 Wen et al.,2018.

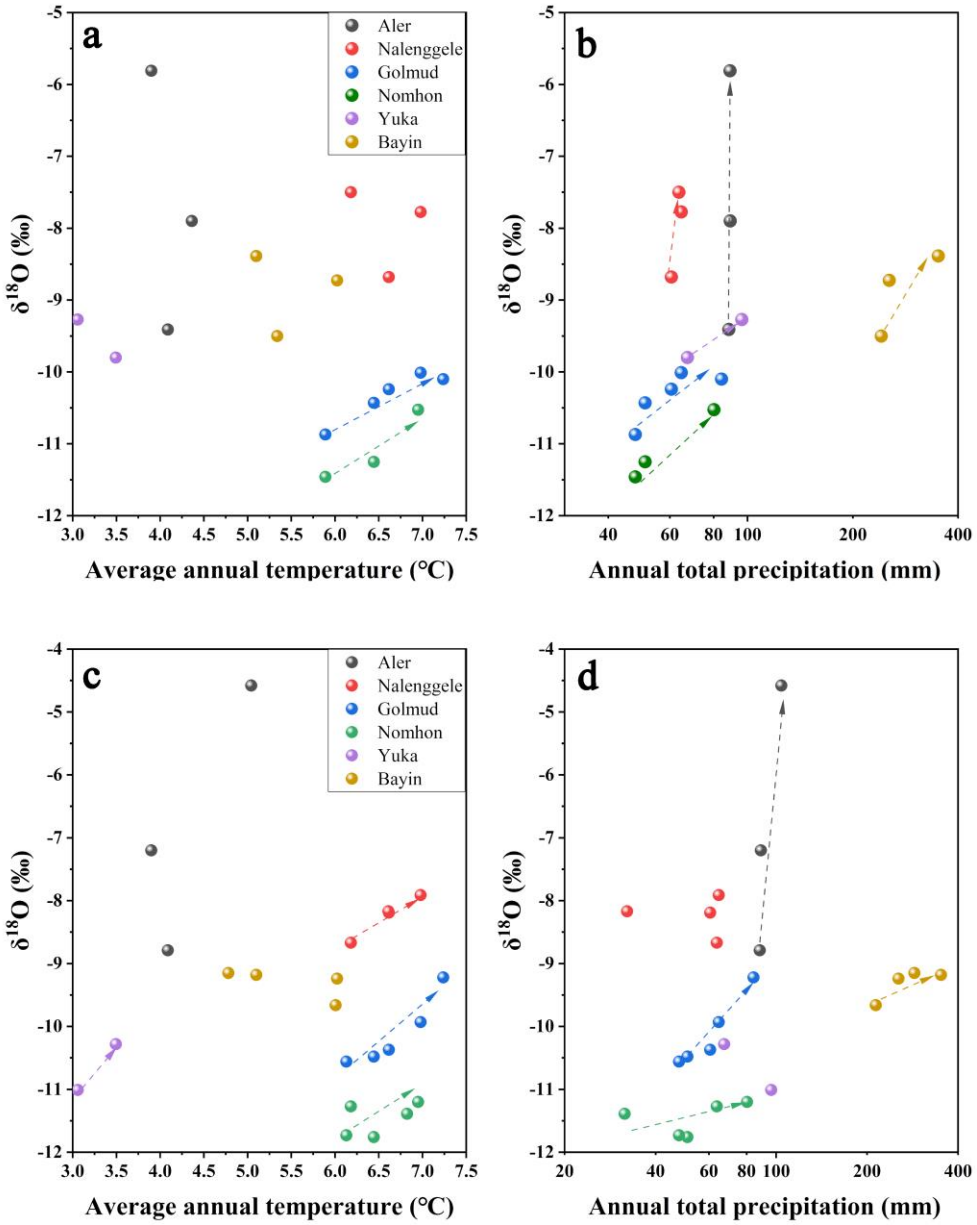


562

563 **Figure 12.** Surface water $\delta^{18}O$ and temperature (a) and precipitation (b); Groundwater $\delta^{18}O$ and temperature (c)
564 and precipitation (d) in the Qaidam Basin. The light lines indicate $\delta^{18}O$ change with temperature and
565 precipitation.

## 6. Conclusion

The spatial and temporal variations of $\delta^{18}O$ and $\delta D$ in surface water and groundwater of the Qaidam Basin reflect their dynamic hydrological responses to climate change, water sources, and local temperature and precipitation regimes, especially precipitation, at interannual and seasonal scales.

(1) The mean values of surface water $\delta^{18}O$ and $\delta D$ in the Eastern Kunlun Mountains gradually decrease eastward, whereas the opposite is true for the Qilian Mountains river system, reflecting the intensity of westerlies moisture transport and the influence of local climatic conditions, respectively. Surface water is enriched in heavy H-O isotopes during wet season and is relatively depleted during dry season. The base flow is maintained by groundwater recharge during dry season, while receiving varying proportions of groundwater (26%–62%), ice/snow meltwater (23%–47%) and precipitation (10%–45%) during wet season. The seasonal isotopic variability is determined by the quantity of precipitation and its gradient in the basin, with precipitation in the Qilian Mountains contributing more to rivers than in the eastern Kunlun Mountains.

(2) The key factor accelerating groundwater circulation in the Qaidam Basin is the contribution of precipitation and meltwater produced by climate change. The groundwater systems located in the collision and convergence zone of several mountain ranges are distinguished by enriched H-O isotopes during wet season, high $^{3}H$ concentrations, and marked rapid seasonal recharge. Modern precipitation and meltwater can infiltrate through favorable structural conduits (e.g., large-scale active fault zones), resulting in rapid groundwater recharge. In contrast, the groundwater systems in the western Qilian Mountains and the middle Eastern Kunlun Mountains are depleted in H-O isotopes during wet season and $^{3}H$ concentrations are low, and are primarily slowly recharged by seasonal ice/snow meltwater, which consisted of modern water and submodern water (>60 years). The confined groundwater is considerably depleted in H-O isotopes, and for the most part exhibits imperceptible seasonal changes. $^{3}H$ concentrations are very low, and recharge is quite slow, dominated by fossil water.

(3) Warming climate has exerted a substantial impact on the hydrological processes across the basin, accelerating water cycle and raising water storage uncertainties in the eastern and southwestern basin through the increased precipitation and melting of glaciers and snow. However, this increasing trend of water resources in the basin seems to be unsustainable. The southwestern

basin could suffer a rapid loss in total water resources in the future as precipitation increases and solid water ablation in mountainous areas becoming severely out of balance undergone climatic extreme changes.

## Author Contribution

Conceptualization: Yu Zhang, Hongbing Tan; Funding acquisition: Xiying Zhang; Investigation: Peixin Cong; Resources: Wenbo Rao; Visualization: Dongping Shi; Writing–original draft: Yu Zhang; Writing–review & editing: Hongbing Tan.


## Acknowledgments

This study was financially supported by the National Natural Science Foundation of China (U22A20573), the Fundamental Research Funds for the Central Universities (B230205010), and the Postgraduate Research & Practice Innovation Program of Jiangsu Province (KYCX22_0666). We thank the editors, Prof. Michael K. Stewart and the other two anonymous reviewers for providing a list of critical and very valuable comments that helped to improve the manuscript. We also thank Prof. Beckie, R. D. for writing suggestions and thoughtful reviews with the final revision. We would like to express our gratitude for all members' help both in the field observation and geochemical analysis in the laboratory.


## Declaration of interests

The authors declare that they have no known competing financial interests or personal relationships that could have appeared to influence the work reported in this paper.

## Data Availability Statement

The complete list of isotopes and their values is available in Table S1 in Supporting Information. The meteorological data can be obtained on China Meteorological Data Network (http://data.cma.cn). The monthly mean ERA5 reanalysis data (0.25° × 0.25°) can be obtained from European Centre for Medium-Range Weather Forecasts (ECMWF, https://www.ecmwf.int/).

## References


Ahmed, M., Chen, Y., & Khalil, MM (2022). Isotopic Composition of Groundwater Resources in Arid Environments. Journal of Hydrology, 127773.

623 Bam, EK, Ireson, AM, van Der Kamp, G., & Hendry, JM (2020). Ephemeral ponds: Are they the
624 dominant source of depression-focused groundwater recharge?. Water Resources Research,
625 56(3), e2019WR026640.
626 Befus, KM, Jasechko, S., Luijendijk, E., Gleeson, T., & Bayani Cardenas, M. (2017). The rapid
627 yet uneven turnover of Earth's groundwater. Geophysical Research Letters, 44(11), 5511-
628 5520.
629 Benettin, P., Rodriguez, N. B., Sprenger, M., Kim, M., Klaus, J., Harman, C. J., ... & McDonnell,
630 J. J. (2022). Transit time estimation in catchments: Recent developments and future directions.
631 Water Resources Research, 58(11), e2022WR033096.
632 Beyerle, U., Purtschert, R., Aeschbach-Hertig, W., Imboden, D. M., Loosli, H. H., Wieler, R., &
633 Kipfer, R. (1998). Climate and groundwater recharge during the last glaciation in an ice-
634 covered region. Science, 282(5389), 731-734.
635 Boutt DF, Mabee SB, Yu Q. Multiyear increase in the stable isotopic composition of stream water
636 from groundwater recharge due to extreme precipitation[J]. Geophysical Research Letters,
637 2019, 46(10): 5323-5330.
638 Bowen, GJ, Cai, Z., Fiorella, RP, & Putman, AL (2019). Isotopes in the water cycle: regional-to
639 global-scale patterns and applications. Annual Review of Earth and Planetary Sciences, 47(1).
640 Chang, Q., Ma, R., Sun, Z., Zhou, A., Hu, Y., & Liu, Y. (2018). Using isotopic and geochemical
641 tracers to determine the contribution of glacier-snow meltwater to streamflow in a partly
642 glacierized alpine-gorge catchment in northeastern Qinghai-Tibet Plateau. Journal of
643 Geophysical Research: Atmospheres, 123(18), 10-037.
644 Chatterjee, S., Gusyev, MA, Sinha, UK, Mohokar, HV, & Dash, A. (2019). Understanding water
645 circulation with tritium tracer in the Tural-Rajwadi geothermal area, India. Applied
646 Geochemistry, 109, 104373.
647 Chen, C., Zhang, X., Lu, H., Jin, L., Du, Y., & Chen, F. (2021). Increasing summer precipitation
648 in arid Central Asia linked to the weakening of the East Asian summer monsoon in the recent
649 decades. International Journal of Climatology, 41(2), 1024-1038.
650 Chen, J., Wang Y., Zheng, J., & Cao L. (2019). The changes in the water volume of Ayakekumu
651 Lake based on satellite remote sensing data. Journal of Natural Resources, 34(6), 1331- 1344
652 (in Chinese with English abstract).
653 Clark, I. D., & Fritz, P. (2013). Environmental isotopes in hydrogeology. CRC press.

Condon, LE, Atchley, AL, & Maxwell, RM (2020). Evapotransspiration depletes groundwater under warming over the contiguous United States. Nature communications, 11(1), 1-8.

Craig, H. (1961). Isotopic variations in meteoric waters. Science, 133(3465), 1702-1703.

Cui, Y., LIU, F., & Hao, Q. (2015). Characteristics of hydrogen and oxygen isotopes and renewal of groundwater in the Nuomuhong alluvial fan. Hydrogeology & Engineering Geology, 42(6), 1-7 (in Chinese with English abstract).

Dansgaard, W. (1964). Stable isotopes in precipitation. tellus, 16(4), 436-468.

Durack, PJ, Wijffels, SE, & Matear, RJ (2012). Ocean salinities reveal strong global water cycle intensification during 1950 to 2000. Science, 336(6080), 455-458.

Juan, G., Li, Z., Qi, F., Ruifeng, Y., Tingting, N., Baijuan, Z., ... & Pengfei, L. (2020). Environmental effect and spatiotemporal pattern of stable isotopes in precipitation on the transition zone between the Tibetan Plateau and arid region. Science of The Total Environment, 749, 141559.

Haddeland, I., Heinke, J., Biemans, H., Eisner, S., Flörke, M., Hanasaki, N., ... & Wisser, D. (2014). Global water resources affected by human interventions and climate change. Proceedings of the National Academy of Sciences, 111(9), 3251-3256.

He, Y., Zhao, C., Liu, Z., Wang, H., Liu, W., Yu, Z., ... & Ito, E. (2016). Holocene climate controls on water isotopic variations on the northeastern Tibetan Plateau. Chemical Geology, 440, 239-247.

Hooper, RP (2003). Diagnostic tools for mixing models of stream water chemistry. Water Resources Research, 39(3), 1055.

Hooper, RP, Christophersen, N., & Peters, NE (1990). Modeling streamwater chemistry as a mixture of soilwater end-members—An application to the Panola Mountain catchment, Georgia, USA. Journal of Hydrology, 116(1-4 ), 321-343.

Huntington, TG (2006). Evidence for intensification of the global water cycle: review and synthesis. Journal of Hydrology, 319(1-4), 83-95.

Jasechko, S., Birks, SJ, Gleeson, T., Wada, Y., Fawcett, PJ, Sharp, ZD, ... & Welker, JM (2014). The pronounced seasonality of global groundwater recharge. Water Resources Research, 50(11), 8845-8867.

683 Jasechko, S., Perrone, D., Befus, K. M., Bayani Cardenas, M., Ferguson, G., Gleeson, T., ... &
684 Kirchner, J. W. (2017). Global aquifers dominated by fossil groundwaters but wells
685 vulnerable to modern contamination. Nature Geoscience, 10(6), 425-429.
686 Jiao, JJ, Zhang, X., Liu, Y., & Kuang, X. (2015). Increased water storage in the Qaidam Basin, the
687 North Tibet Plateau from GRACE gravity data. PloS one, 10(10), e0141442.
688 Juan, G., Li, Z., Qi, F., Ruifeng, Y., Tingting, N., Baijuan, Z., … & Pengfei, L. (2020).
689 Environmental effect and spatiotemporal pattern of stable isotopes in precipitation on the
690 transition zone between the Tibetan Plateau and arid region. Science of The Total
691 Environment, 749, 141559.
692 Kang, S., Cong, Z., Wang, X., Zhang, Q., Ji, Z., Zhang, Y., & Xu, B. (2019). The transboundary
693 transport of air pollutants and their environmental impacts on Tibetan Plateau. Chinese
694 Science Bulletin, 64(27), 2876-2884.
695 Ke, L., Song, C., Wang, J., Sheng, Y., Ding, X., Yong, B., ... & Luo, S. (2022). Constraining the
696 contribution of glacier mass balance to the Tibetan lake growth in the early 21st century.
697 Remote Sensing of Environment, 268, 112779.
698 Kong, Y., Wang, K., Pu, T., & Shi, X. (2019). Nonmonsoon precipitation dominates groundwater
699 recharge beneath a monsoon-affected glacier in Tibetan Plateau. Journal of Geophysical
700 Research: Atmospheres, 124(20), 10913-10930.
701 Kuang, X., & Jiao, JJ (2016). Review on climate change on the Tibetan Plateau during the last half
702 century. Journal of Geophysical Research: Atmospheres, 121(8), 3979-4007.
703 Li, L., & Garzione, CN (2017). Spatial distribution and controlling factors of stable isotopes in
704 meteoric waters on the Tibetan Plateau: Implications for paleoelevation reconstruction. Earth
705 and Planetary Science Letters, 460, 302-314.
706 Li, L., Shen, H., Li, H., & Xiao, J. (2015). Regional differences of climate change in Qaidam Basin
707 and its contributing factors. Journal of Natural Resources, 30, 641-650 (in Chinese with
708 English abstract).
709 Liu, F., Cui, Y., Zhang, G., Geng, F., & Liu, J. (2014). Using the 3H and 14C dating methods to
710 calculate the groundwater age in Nuomuhong, Qaidam Basin. Geoscience, 28 (6), 1322-1328
711 (in Chinese with English abstract).

712 Liu, J., Song, X., Sun, X., Yuan, G., Liu, X., & Wang, S. (2009). Isotopic composition of
713 precipitation over Arid Northwestern China and its implications for the water vapor origin.
714 Journal of Geographical Sciences, 19(2), 164-174 (in Chinese with English abstract).
715 Ma, J., Ding, Z., Edmunds, W. M., Gates, J. B., & Huang, T. (2009). Limits to recharge of
716 groundwater from Tibetan plateau to the Gobi desert, implications for water management in
717 the mountain front. Journal of Hydrology, 364(1-2), 128-141.
718 Malard, A., Sinreich, M., & Jeannin, PY (2016). A novel approach for estimating karst
719 groundwater recharge in mountainous regions and its application in Switzerland.
720 Hydrological Processes, 30(13), 2153-2166.
721 Masson-Delmotte, V., Zhai, P., Pirani, A., Connors, SL, Péan, C., Berger, S., ... & Zhou, B. (2021).
722 Climate change 2021: the physical science basis. Contribution of working group I to the sixth
723 assessment report of the intergovernmental panel on climate change, 2.
724 Moran, BJ, Boutt, DF, & Munk, LA (2019). Stable and radioisotope systematics reveal fossil water
725 as fundamental characteristic of arid orogenic-scale groundwater systems. Water Resources
726 Research, 55(12), 11295-11315.
727 Parnell, AC, Inger, R., Bearhop, S., & Jackson, AL (2010). Source partitioning using stable
728 isotopes: coping with too much variation. PloS one, 5(3), e9672.
729 Rodriguez, N. B., Pfister, L., Zehe, E., & Klaus, J. (2021). A comparison of catchment travel times
730 and storage deduced from deuterium and tritium tracers using StorAge Selection functions.
731 Hydrology and Earth System Sciences, 25(1), 401-428.
732 Shen, C., Jia, L., & Ren, S. (2022). Inter-and Intra-Annual Glacier Elevation Change in High
733 Mountain Asia Region Based on ICESat-1&2 Data Using Elevation-Aspect Bin Analysis
734 Method. Remote Sensing, 14(7), 1630.
735 Shi, D., Tan, H., Chen, X., Rao, W., & Basang, R. (2021). Uncovering the mechanisms of seasonal
736 river–groundwater circulation using isotopes and water chemistry in the middle reaches of
737 the Yarlungzangbo River, Tibet. Journal of Hydrology, 603, 127010.
738 Song, C., Huang, B., Richards, K., Ke, L., & Hien Phan, V. (2014). Accelerated lake expansion
739 on the Tibetan Plateau in the 2000s: Induced by glacial melting or other processes?. Water
740 Resources Research, 50(4), 3170-3186.
741 Stewart, M. K., Morgenstern, U., Gusyev, M. A., & Małoszewski, P. (2017). Aggregation effects
742 on tritium-based mean transit times and young water fractions in spatially heterogeneous

743 catchments and groundwater systems. Hydrology and Earth System Sciences, 21(9), 4615-
744 4627.
745 Tan, H., Chen, J., Rao, W., Zhang, W., & Zhou, H. (2012). Geothermal constraints on enrichment
746 of boron and lithium in salt lakes: An example from a river-salt lake system on the northern
747 slope of the eastern Kunlun Mountains, China. Journal of Asian Earth Sciences, 51, 21-29.
748 Tan, H., Rao, W., Chen, J., Su, Z., Sun, X., & Liu, X. (2009). Chemical and isotopic approach to
749 groundwater cycle in western Qaidam Basin, China. Chinese Geographical Science, 19, 357-
750 364.
751 Tan, H., Zhang, Y., Rao, W., Guo, H., Ta, W., Lu, S., & Cong, P. (2021). Rapid groundwater
752 circulation inferred from temporal water dynamics and isotopes in an arid system.
753 Hydrological Processes, 35(6), e14225.
754 Tian, L., Yao, T., Sun, W., Stievenard, M., & Jouzel, J. (2001). Relationship between δD and δ18O
755 in precipitation on north and south of the Tibetan Plateau and moisture recycling. Science in
756 China Series D: Earth Sciences, 44(9), 789-796.
757 Wang, L., Yao, T., Chai, C., Cuo, L., Su, F., Zhang, F., Yao, Z., Zhang, Y., Li, X., Qi, J., Hu, Z.,
758 Liu, J., & Wang, Y. (2021). TP-River: Monitoring and Quantifying Total River Runoff from
759 the Third Pole, Bulletin of the American Meteorological Society, 102(5), E948-E965.
760 Wang, S., Lei, S., Zhang, M., Hughes, C., Crawford, J., Liu, Z., & Qu, D. (2022). Spatial and
761 seasonal isotope variability in precipitation across China: Monthly isoscapes based on
762 regionalized fuzzy clustering. Journal of Climate, 35(11), 3411-3425.
763 Wang, S., Zhang, M., Che, Y., Chen, F., & Qiang, F. (2016). Contribution of recycled moisture to
764 precipitation in oases of arid central Asia: A stable isotope approach. Water Resources
765 Research, 52(4), 3246-3257.
766 Wang, T., Yang, D., Yang, Y., Zheng, G., Jin, H., Li, X., ... & Cheng, G. (2023). Unsustainable
767 water supply from thawing permafrost on the Tibetan Plateau in a changing climate. Science
768 bulletin, S2095-9273.
769 Wang, X., Chen, M., Gong, P., & Wang, C. (2019). Perfluorinated alkyl substances in snow as an
770 atmospheric tracer for tracking the interactions between westerly winds and the Indian
771 Monsoon over western China. Environment international, 124, 294-301.

Wang, X., Yang, M., Liang, X., Pang, G., Wan, G., Chen, X., & Luo, X. (2014). The dramatic climate warming in the Qaidam Basin, northeastern Tibet Plateau, during 1961–2010. International Journal of Climatology, 34(5), 1524-1537.

Wang, Y., Guo, H., Li, J., Huang, Y., Liu, Z., Liu, C., Guo, X., Zhou, J., Shang, X., Li, J., Zhuang, Y., & Cheng, H. (2008). Investigation and assessment of groundwater resources and their environmental issues in the Qaidam Basin. Geological Publishing House, Beijing (in Chinese).

Wei, L., Jiang, S., Ren, L., Tan, H., Ta, W., Liu, Y., ... & Duan, Z. (2021). Spatiotemporal changes of terrestrial water storage and possible causes in the closed Qaidam Basin, China using GRACE and GRACE Follow-On data. Journal of Hydrology, 598, 126274.

Wen, G., Wang, W., Duan, L., Gu, X., Li, Y., & Zhao, J. (2018). Quantitatively evaluating exchanging relationship between river water and groundwater in Bayin River Basin of northwest China using hydrochemistry and stable isotope. Arid Land Geography, 41, 734-743 (in Chinese with English abstract).

Wu, H., Zhang, C., Li, XY, Fu, C., Wu, H., Wang, P., & Liu, J. (2022). Hydrometeorological Processes and Moisture Sources in the Northeastern Tibetan Plateau: Insights from a 7-Yr Study on Precipitation Isotopes. Journal of Climate, 35(20), 2919-2931.

Xiang, L., Wang, H., Steffen, H., Wu, P., Jia, L., Jiang, L., & Shen, Q. (2016). Groundwater storage changes in the Tibetan Plateau and adjacent areas revealed from GRACE satellite gravity data. Earth and Planetary Science Letters, 449, 228-239.

Xiao, Y., Shao, J., Cui, Y., Zhang, G., & Zhang, Q. (2017). Groundwater circulation and hydrogeochemical evolution in Nomhon of Qaidam Basin, northwest China. Journal of Earth System Science, 126 (2), 1-16.

Xiao, Y., Shao, J., Frape, SK, Cui, Y., Dang, X., Wang, S., & Ji, Y. (2018). Groundwater origin, flow regime and geochemical evolution in arid endorheic watersheds: a case study from the Qaidam Basin, northwestern China. Hydrology and Earth System Sciences, 22(8), 4381-4400.

Xu, W., Su, X., Dai, Z., Yang, F., Zhu, P., & Huang, Y. (2017). Multi-tracer investigation of river and groundwater interactions: a case study in Nalenggele River basin, northwest China. Hydrogeology Journal, 25(7), 2015-2029.

Yang, N., & Wang, G. (2020). Moisture sources and climate evolution during the last 30 kyr in northeastern Tibetan Plateau: Insights from groundwater isotopes (2H, 18O, 3H and 14C) and water vapor trajectories modeling. Quaternary Science Reviews, 242, 106426.

Yang, N., Wang, G., Liao, F., Dang, X., & Gu, X. (2023). Insights into moisture sources and evolution from groundwater isotopes (2H, 18O, and 14C) in Northeastern Qaidam Basin, Northeast Tibetan Plateau, China. Science of The Total Environment, 864, 160981.

Yang, N., Zhou, P., Wang, G., Zhang, B., Shi, Z., Liao, F., ... & Gu, X. (2021). Hydrochemical and isotopic interpretation of interactions between surfaces water and groundwater in Delingha, Northwest China. Journal of Hydrology, 598, 126243.

Yang, Y., Wu, Q., & Jin, H. (2016). Evolutions of water stable isotopes and the contributions of cryosphere to the alpine river on the Tibetan Plateau. Environmental Earth Sciences, 75(1), 1-11.

Yao, T., Bolch, T., Chen, D., Gao, J., Immerzeel, W., Piao, S., ... & Zhao, P. (2022). The imbalance of the Asian water tower. Nature Reviews Earth & Environment, 1-15.

Yao, T., Masson-Delmotte, V., Gao, J., Yu, W., Yang, X., Risi, C., ... & Hou, S. (2013). A review of climatic controls on δ18O in precipitation over the Tibetan Plateau: Observations and simulations. Reviews of Geophysics, 51(4), 525-548.

Ye, C., Zheng, M., Wang, Z., Hao, W., Wang, J., Lin, X., & Han, J. (2015). Hydrochemical characteristics and sources of brines in the Gasikule salt lake, Northwest Qaidam Basin, China. Geochemical Journal, 49(5), 481-494.

Zhang, G., Yao, T., Shum, CK, Yi, S., Yang, K., Xie, H., ... & Yu, J. (2017). Lake volume and groundwater storage variations in Tibetan Plateau's endorheic basin. Geophysical Research Letters, 44(11), 5550-5560.

Zhang, Q., Zhu, B., Yang, J., Ma, P., Liu, X., Lu, G., ... & Wang, D. (2021). New characteristics about the climate humidity trend in Northwest China. Chinese Science Bulletin, 66, 3757-3771.

Zhang, X., Chen, J., Chen, J., Ma, F., & Wang, T. (2022). Lake Expansion under the Groundwater Contribution in Qaidam Basin, China. Remote Sensing, 14(7), 1756 .

Zhao, D., Wang, G., Liao, F., Yang, N., Jiang, W., Guo, L., ... & Shi, Z. (2018). Groundwater-surface water interactions derived by hydrochemical and isotopic (222Rn, deuterium, oxygen-18) tracers in the Nomhon area, Qaidam Basin, NW China. Journal of Hydrology, 565, 650-661.

Zhao, D., Wang, G., Liao, F., Yang, N., Jiang, W., Guo, L., … & Shi, Z. (2018). Groundwater-surface water interactions derived by hydrochemical and isotopic (222Rn, deuterium,

834 oxygen-18) tracers in the Nomhon area, Qaidam Basin, NW China. Journal of Hydrology,
835 565, 650-661.
836 Zhao, L., Yin, L., Xiao, H., Cheng, G., Zhou, M., Yang, Y., ... & Zhou, J. (2011). of surface runoff
837 in the headwaters of the Heihe River basin. Chinese Science Bulletin, 56(4), 406-415.
838 Zhu, G., Liu, Y., Wang, L., Sang, L., Zhao, K., Zhang, Z., ... & Qiu, D. (2023). The isotopes of
839 precipitation have climate change signal in arid Central Asia. Global and Planetary Change,
840 225, 104103.
841 Zhu, J., Chen, H., & Gong, G. (2015). Hydrogen and oxygen isotopic compositions of precipitation
842 and its water vapor sources in Eastern Qaidam Basin. Environmental Science, 36(8), 2784-
843 2790 (in Chinese with English abstract).
844 Zhu, P. (2015). Groundwater circulation patterns of Yuqia-Maihai Basin in the middle and lower
845 reaches of Yuqia River. Doctoral dissertation, Jilin University, Changchun (in Chinese with
846 English abstract).
847 Zou, Y., Kuang, X., Feng, Y., Jiao, JJ, Liu, J., Wang, C., ... & Zheng, C. (2022). Solid water melt
848 dominates the increase of total groundwater storage in the Tibetan Plateau. Geophysical
849 Research Letters, e2022GL100092.